Front. Chem. Sci. Eng. 2022, 16(6): 838–853
https://doi.org/10.1007/s11705-021-2129-8

REVIEW ARTICLE

Interfacial induction and regulation for microscale crystallization process: a critical review

Mengyuan Wu, Zhijie Yuan, Yuchao Niu, Yingshuang Meng, Gaohong He, Xiaobin Jiang (✉)

State Key Laboratory of Fine Chemicals, School of Chemical Engineering, Dalian University of Technology, Dalian 116024, China

Abstract Microscale crystallization is at the frontier of chemical engineering, material science, and biochemical research and is affected by many factors. The precise regulation and control of microscale crystal processes is still a major challenge. In the heterogeneous induced nucleation process, the chemical and micro/nanostructural characteristics of the interface play a dominant role. Ideal crystal products can be obtained by modifying the interface characteristics, which has been proven to be a promising strategy. This review illustrates the application of interface properties, including chemical characteristics (hydrophobicity and functional groups) and the morphology of micro/nanostructures (rough structure and cavities, pore shape and pore size, surface porosity, channels), in various microscale crystallization controls and process intensification. Finally, possible future research and development directions are outlined to emphasize the importance of interfacial crystallization control and regulation for crystal engineering.

Keywords interfacial crystallization, heterogeneous nucleation, supersaturation, micro/nanostructure, process control and intensification

1 Introduction

Crystallization is one of the most important unit operations in the chemical industry [1]. In the pharmaceutical industry, 85% of solid production depends on the crystallization process. In principle, nucleation, which determines the crystal properties, is the key step for controlling crystallization. Controlling crystallization is highly important in many scientific and technical fields, including environmental engineering, pharmaceutical engineering, semiconductors, food products, nutraceuticals, and minerals in biological and synthetic systems [2]. However, nucleation is easily induced by external interfaces in most practical circumstances; such external interfaces are known as heterogeneous interfaces, and nucleation induced by these interfaces is extremely difficult to control. The microstructure of the heterogeneous nucleation interface plays an important role in controlling heterogeneous nucleation, which has made great progress in the last decade [3]. Various interface materials have been developed to induce the heterogeneous nucleation of crystals in the metastable region to obtain crystals with larger sizes and that are more suitable for diffraction [4]. Therefore, determining the mechanism by which the interface structure regulates the heterogeneous nucleation process is of great significance for obtaining high-quality crystal products and realizing the directional preparation of crystals with special morphology. The heterogeneously induced nucleation process is affected by the chemical properties and micro/nanostructures of the interface, including hydrophobicity, functional groups, rough structure and cavities, pore shape and pore size, surface porosity, and channels, as shown in Fig. 1.

Herein, the roles of the interfacial chemical properties and micro/nanostructures in controlling nucleation and crystallization are reviewed from the atomic scale to the micro/nanoscale; this review lays a foundation for realizing controllable crystallization and the directional preparation of crystalline products. Research on crystallization based on interface characteristics has important applications not only in the fields of medicine, food and mineralization, which use crystallization in current practice but also in the future development of new material technologies and process engineering, including the directional design of new materials such as metal-organic frameworks and covalent organic frameworks, drug carriers, vaccine preparation and other major fields related to life and health.

Received July 1, 2021; accepted October 15, 2021

E-mail: xbjiang@dlut.edu.cn

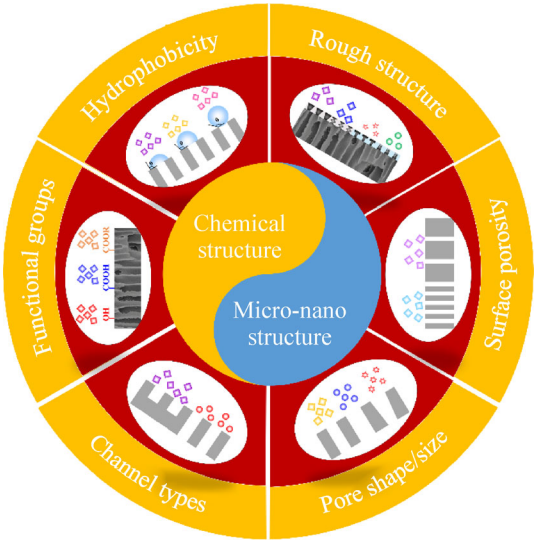

Fig. 1 Effect of physicochemical microstructure on the interfacial based microscale crystallization.

2 Nucleation theory

2.1 Thermodynamics-nucleation barrier

The nucleation energy of a system is the key to determining whether the crystal nucleates, though the energy is difficult to calculate, so the nucleation barrier is introduced to judge the crystal growth. The nucleation barrier is determined by the complex interactions between physical and chemical parameters. The influence of the porous interface on the reduction of the nucleation barrier can be quantified by an interfacial correlation factor ($f(\theta)$), which is defined as [5]:

$$f(\theta)=\frac{\Delta G^{*}_{\text{Heter}}}{\Delta G^{*}_{\text{Homo}}}=\frac{(2+\cos\ \theta)(1-\cos\ \theta)^{2}}{4}\left[1-\varepsilon\frac{(1+\cos\ \theta)^{2}}{(1-\cos\ \theta)^{2}}\right]^{3}, \tag{1}$$

where $\Delta G^{*}_{\text{Homo}}$ and $\Delta G^{*}_{\text{Heter}}$ are the homogeneous nucleation barrier ($\text{kJ}\cdot\text{mol}^{-1}$) and heterogeneous nucleation barrier ($\text{kJ}\cdot\text{mol}^{-1}$), respectively, and ε is the surface porosity, which is defined as the ratio of the total pore areas ($\sum A_{\text{p}}$) on the whole geometrical surface A of the interface. $f(\theta)$ is the interface correlation coefficient, which indicates a reduction in the nucleation barrier due to the presence of rough porous surfaces. θ is the apparent contact angle (°) and is influenced by the intrinsic hydrophobicity and roughness of the interface. The wetting behavior of rough surfaces is usually described by the Wenzel equation [6]:

$$(\gamma_{\text{sf}}-\gamma_{\text{sc}})/\gamma_{\text{cf}}=\frac{1}{r}\cos\ \theta, \tag{2}$$

where r is the roughness area ratio.

For $\varepsilon = 1$, $r = 1$ and $\theta = 180°$, the crystallization is considered to be in a homogeneous phase, and $f(\theta)$ is 1. For $\varepsilon = 0$, Eq. (1) reduces to the classical value for heterogeneous nucleation on a nonporous interface, which is defined as [5]:

$$f(\theta)=\frac{\Delta G^{*}_{\text{Heter}}}{\Delta G^{*}_{\text{Homo}}}=\frac{(2+\cos\ \theta)(1-\cos\ \theta)^{2}}{4}. \tag{3}$$

According to nucleation theory, the system can cross the nuclear energy barrier and nucleate immediately by changing the physicochemical structure of the heterogeneous nucleation interface.

2.2 Kinetics — nucleation rate

Classical nucleation theory mainly describes and predicts the nucleation process of crystals, involving crystallization time, nucleation rate and other related physical quantities. The rate of nucleation is related to the state of nucleation and plays a key role after the system reaches the supersaturated concentration. The nucleation rate in a homogeneous system is qualitatively determined by the Eq. (4) [7]:

$$\begin{aligned}J_{\text{Nucle}}&=A\ \exp\left[-\frac{\Delta G^{*}_{\text{Homo}}}{\kappa T}\right]\\&=A\ \exp\left[-\frac{16\pi\gamma^{3}V_{\text{m}}^{2}}{3\kappa^{3}T^{3}(\ln\ S)^{2}}\right],\end{aligned} \tag{4}$$

where J is the nucleation rate; A refers to the pre-factor; γ, V_{m}, κ, T and S are the surface tension ($\text{J}\cdot\text{m}^{-2}$), molecular volume ($\text{cm}^{3}\cdot\text{mol}^{-1}$), Boltzmann constant, temperature (K), and supersaturation, respectively. Similarly, the change in the nucleation barrier on the porous interface could also affect the nucleation rate. The nucleation barrier formula of the porous interface is determined by $f(\theta)$.

$$\begin{aligned}J&=A\ \exp\left[-\frac{\Delta G^{*}_{\text{Heter}}}{\kappa T}\right]\\&=A\ \exp\left[-f(\theta)\frac{16\pi\gamma^{3}V_{\text{m}}^{2}}{3\kappa^{3}T^{3}(\ln\ S)^{2}}\right].\end{aligned} \tag{5}$$

The nucleation rate is closely related not only to the solution itself but also to external influences.

3 Effect of interface properties on crystallization

The microstructure of heterogeneous nucleation interface plays an important role in controlling heterogeneous nucleation; knowledge of such interfaces has greatly progressed over the last decade. In general, the hetero-

geneous induced nucleation process can be summarized as follows: 1) interfaces with diverse chemical properties, such as hydrophobicity and electrostatic-induced nucleation by functional groups, promote the heterogeneous nucleation of crystals; 2) the heterogeneous nucleation of crystals is affected by the interface micro/nanostructures, such as rough structures and cavities, pore shape and pore size, surface porosity and channels.

3.1 Hydrophobicity

Interface chemistry is fundamental to crystallization regulation and controls crystallization at the atomic level. Hydrophobic solvents are have specific chemical properties at the interface, and superhydrophobic solvent interfaces are ideal platforms for crystallization design, as they help to regulate the proportion of solvent (such as water) in the interface, adjust the interactions between the interface and the crystalline components, and change the nuclear energy barriers of crystals, as shown in Eq. (1). According to the formula of $\Delta G^*_{\text{Heter}}$ at porous surfaces, the nucleation barrier at different material interfaces is shown in Fig. 2. With increasing θ ranging from 0° (superhydrophilic) to 180° (superhydrophobic), the correlation coefficient of the nuclear barrier interface increases gradually (Fig. 2(a)), which means that the nucleation process can be controlled by changing the interfacial hydrophobicity.

With great progress in membrane science, membrane distillation crystallization (MDC) has great significance in generating crystal products with ideal grain size distributions and in the construction of specific crystal superstructures [8–10]. Superhydrophobic membranes are the most commonly used membranes in MD and include polyvinylidene fluoride (PVDF) [11], polytetrafluoroethylene [12,13], and polypropylene [14,15]. The microporous hydrophobic membrane used in MDC can be used not only as a mass transfer device for solvent concentration but also as a heterogeneous nucleation interface. In practice, the poor hydrophobicity of the membrane leads to a decrease in salt rejection and surface scaling and seriously damage the performance of the membrane. Therefore, the hydrophobicity of the membrane material is the key to ensuring the normal operation of the MD process. Multiple rough structures could form a Cassie-Baxter state on the membrane surface and form a large number of air gaps between the membrane surface and droplets, which could not only improve the hydrophobicity but also effectively

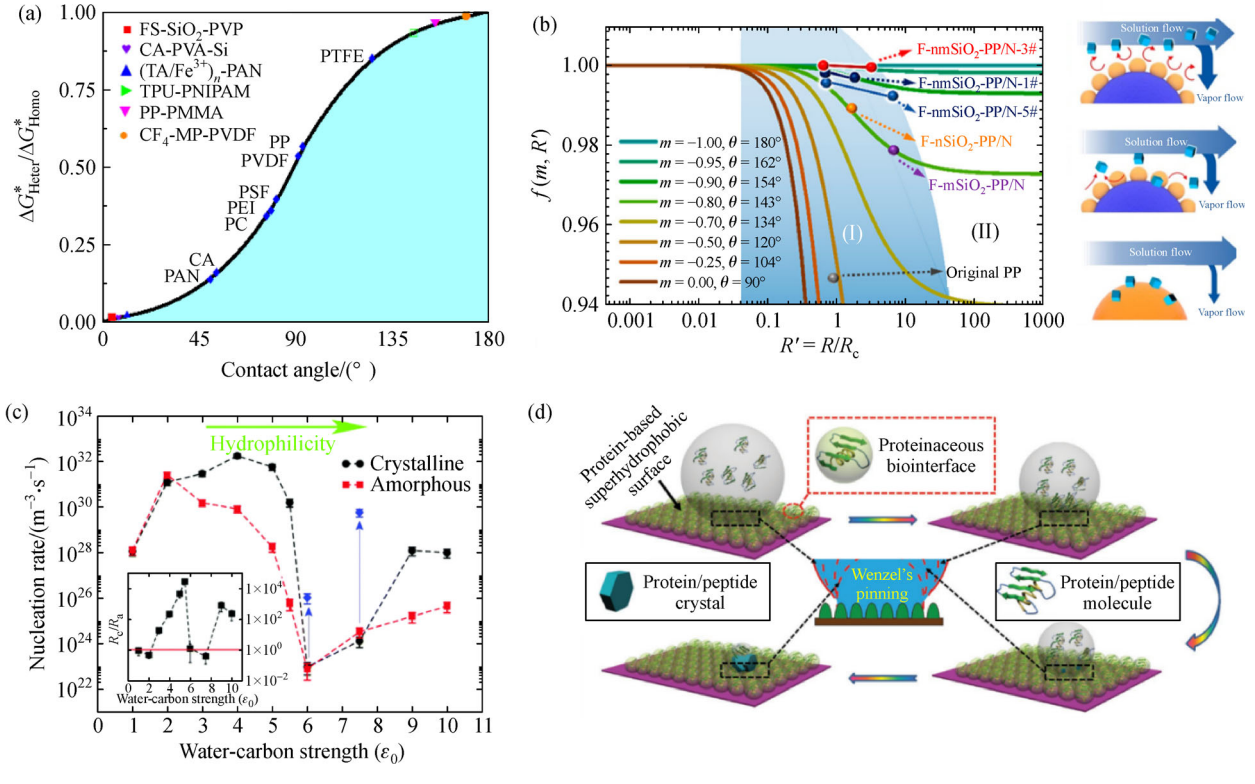

Fig. 2 (a) The nucleation barrier at different material interface with contact angle range from 0° (superhydrophilic) to 180° (superhydrophobic). (b) The interfacial correlation factor $f(m,R')$ of the different fabricated membrane with diverse interfacial micro/nano-structure. Reprinted with permission from ref. [2], copyright 2020, American Chemical Society. (c) Variation of the calculated ice nucleation rates with water-carbon interaction strength. Reprinted with permission from ref. [3], copyright 2016, American Chemical Society. (d) Crystallization of biomolecules on protein-based superhydrophobic surface. Reprinted with permission from ref. [4], copyright 2018, Wiley.

reduce the contact area between the solution and interface, thus reducing the probability of salt ion crystallization and improving the antifouling ability. In addition, according to the "surface slip" theory, the construction of a rough structure could cause an air gap between the solution and the interface, strengthening the hydrophobicity. The crystals formed in the host solution could be transported with the fluid flow to avoid the deposition of particles on the surface. According to thermodynamics (Eq. (1)), optimizing the rough structure and improving the nuclear energy barrier of the interface can effectively prevent interface nucleation and inhibit scaling. Jiang et al. constructed a novel type of MD membrane with a bioinspired micro/nanostructure [2]. According to a hydrodynamics simulation, the bioinspired membrane was highly hydrophobic, achieving the biomimetic functions of lotus leaves and effectively hindering nucleation at the interface (Fig. 2(b)). In addition, the environment at the interface (solution chemistry, temperature) also strongly affected the crystal nucleation and growth. In the MDC process, due to the vaporization of volatile components in the boundary layer, the temperature and concentration of the feed liquid at the boundary are lower and higher than those of the main solution, resulting in temperature and concentration polarization, local explosive nucleation and low-quality crystalline products.

Similar to the crystallization of inorganic salts, interfacial hydrophobicity could significantly change the ice nucleation rate and form different ice surfaces [16]. Compared with hydrophobic interfaces, hydrophilic interfaces more easily attract water molecules, resulting in an increase in the ice nucleation rate, which is attributed to the promotion of heterogeneous ice nucleation on the hydrophilic interface, which has a high surface energy [17,18]. Molecular simulation proved that the enhancement of the binding affinity of water molecules on the interface increased the ice nucleation rate by three orders of magnitude (Fig. 2(c)) [3]. The decrease in surface energy could effectively shorten the residence time of water, resulting in longer nucleation times and a decrease in the ice nucleation rate; therefore, hydrophobic materials are commonly used as anti-freezing substrates [17,19,20].

Protein crystallization is a complex process that is important to the study of protein structure and drug design. Promoting crystal nucleation is a key step in solving the crystallization bottleneck of macromolecular substances such as proteins. Hydrophobic interactions are relatively weak noncovalent interactions between nonpolar molecules, and these hydrophobic residues can aggregate without boiling water in aqueous environments. As shown in Fig. 2(d), the development of interfacial hydrophobicity mainly involves the introduction of low surface energy segments or rough structures, which could interact with proteins and adsorb on the interface, thereby increasing the local concentration of protein molecules and affecting the nucleation rate of the macromolecular crystallization system [4]. The hydrophobic interface helps to form clusters for crystallization until the clusters are stabilized by the heterogeneous interface, inducing the nucleation of insoluble crystals such as proteins [21]. Nanev reported that a hydrophobic coating of dimethylsilane resulted in a high nucleation probability of lysozyme and ferritin due to high nonspecific electrostatic attraction [22–24]. A superhydrophobic biological interface induced protein crystallization through modification of multiple functional hydrophobic groups and micro/nanostructures. Pham et al. prepared hydrophobic self-assembled monolayers by adsorbing undecyl mercaptan, dodecyl mercaptan and octadecyl mercaptan onto transparent gold-plated glass [25]. Compared with traditional commercial cover glass, the self-assembled monolayers showed a faster nucleation rate, larger crystal size and a wider range of crystallization conditions. In addition, this research showed that horse hair could promote protein crystal nucleation due to the surface, which hydrophobically interacted with the proteins in the oils on the horse hair, thus inducing protein crystal nucleation [26].

Based on the theory of hydrophobic surfaces, hydrophobic separation membranes can be obtained by reducing the surface free energy of membrane materials and constructing rough surface structures [27]. The former can introduce substances with low surface free energy, such as fluorine-containing [28] or silicon groups [29], which can be constructed mainly by template methods [30,31], phase separation [32], surface grafting [33] and surface coating [34] (Fig. 3). The latter can enhance the hydrophobicity through changes in the surface roughness. At present, there are many effective methods of constructing rough hydrophobic interfaces, such as the sol-gel method [15], chemical vapor deposition (CVD) [35], vacuum-assisted self-assembly (VASA) [36] and surface coating [37] (Fig. 3).

3.2 Functional groups

The unique chemical interactions between the interface and the crystal molecules could change the solute concentration more generally than hydrophobic interactions at the interface; thus, they are another key factor in controlling the kinetics and thermodynamics of nucleation [38]. During crystallization, polarization determines the excellent adsorption capacity of the solute on the surface of the nucleating agent when the solute and solvent have similar polarities, resulting in surface-induced nucleation. In addition, the surface–solute interaction increases the solute concentration at the interface, and molecular recognition between the surface and solute leads to the partial arrangement of solute-rich layers, also resulting in promoted nucleation [39]. The specific interactions that govern nucleation behavior mainly include hydrogen bonding and ionic bonds [40–43]. As shown in Fig. 4, the type and distribution of interfacial functional groups

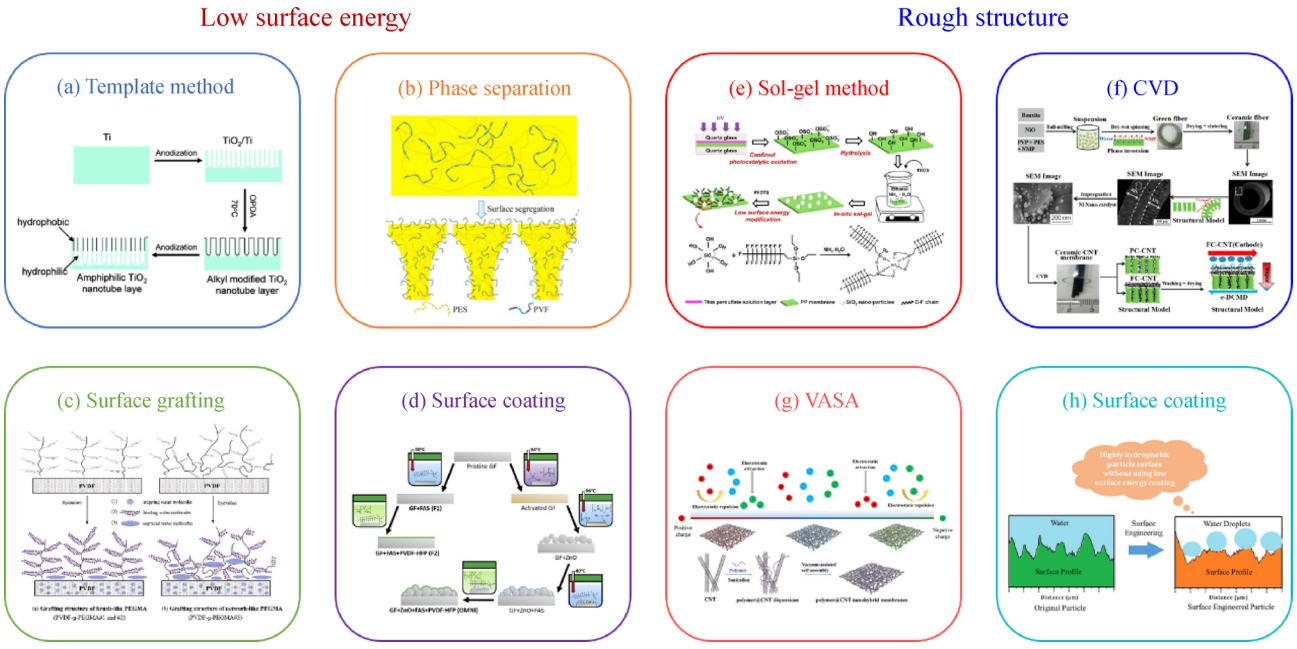

Fig. 3 Hydrophobic interface construction methods. Low surface energy ((a) Template method. Reprinted with permission from ref. [31], copyright 2009, American Chemical Society. (b) Phase separation. Reprinted with permission from ref. [32], copyright 2016, Elsevier. (c) Surface grafting. Reprinted with permission from ref. [33], copyright 2009, Elsevier. (d) Surface coating. Reprinted with permission from ref. [34], copyright 2018, Elsevier). Rough structure ((e) Sol-gel method. Reprinted with permission from ref. [15], copyright 2019, Elsevier. (f) CVD. Reprinted with permission from ref. [35], copyright 2018, American Chemical Society. (g) VASA. Reprinted with permission from ref. [36], copyright 2017, Elsevier. (h) Surface coating. Reprinted with permission from ref. [37], copyright 2020, Elsevier).

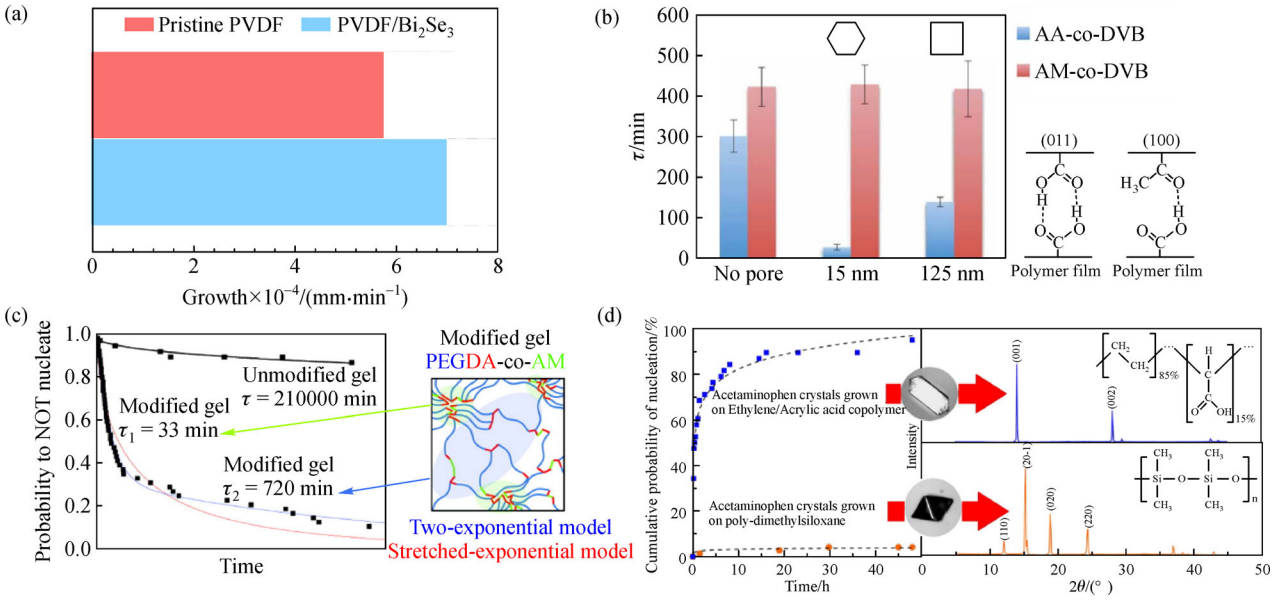

Fig. 4 (a) Growth rates of crystals on the pristine and Bi_2Se_3-modified PVDF membranes. Reprinted with permission from ref. [44], copyright 2018, Royal Society of Chemistry. (b) Effect of polymer surface chemistry on the kinetics of angular nanopore-induced nucleation of aspirin: acrylic acid (AA)-co-crosslinker divinylbenzene (DVB) versus acryloyl morpholine (AM)-co-DVB; proposed aspirin-polymer interactions at the crystal-polymer interface. Reprinted with permission from ref. [47], copyright 2011, Nature Publishing Group. (c) Effect of poly(ethylene glycol) diacrylate-co-AM microgels on nucleation induction time statistics for aspirin. Reprinted with permission from ref. [48], copyright 2011, American Chemical Society. (d) Percentage of samples/vials crystallized on different polymeric surfaces as a function of time. Reprinted with permission from ref. [39], copyright 2014, American Chemical Society.

can control the heterogeneous crystallization process, which is of great significance for practical applications and theoretical research.

The interface with ionizable groups could significantly affect the crystallization of inorganic salts due to the strong polarity, and the crystallization process could also be driven by external static electricity. Macedonio et al. added Bi_2Se_3 into PVDF membranes to accelerate the growth of NaCl crystals and improve the uniformity of the crystal size (Fig. 4(a)) [44]. The surface of the Bi_2Se_3 crystal easily forms a vacancy, which is conducive to the extraction of water molecules from the ion nucleus, thus accelerating the interactions between ions and the formation of crystals.

Protein molecules with hydrophobic and hydrophilic segments could interact with different types of functional groups, which means that the crystallization of macromolecules is more dependent on the interfacial chemical properties than that of inorganic salts [45]. The chemical properties of the interface have a significant effect on crystallization at low protein concentrations [46]. Diao et al. synthesized polymer films with different interfacial chemical properties by a crosslinking method to study the mechanism of interfacial chemistry on the heterogeneous nucleation of aspirin [47]. As shown in Fig. 4(b), the interaction between the polymer film and solute could effectively shorten the induction time of aspirin, which was attributed to the fact that the carboxyl and carbonyl groups of the aspirin reacted with the carboxyl groups on the surface to form hydrogen bonds, inducing preferred orientation nucleation and the growth of aspirin crystals. In addition, polymer microgels with tunable chemical surface structures were also reported by Diao's group to investigate the intermolecular interactions limiting nucleation and controlling crystallization, resulting in an enhancement of nucleation kinetics by four orders of magnitude (Fig. 4(c)) [48]. The polymer matrix enhanced the effective solute–solute interactions and promoted the molecular alignment inferred from preferred crystal orientations on the polymer surfaces, thus inducing rapid nucleation [48,49]. The polymer–solute interactions controlled the nucleation kinetics and promoted nucleation of the pure stable form (Fig. 4(d)) [39]. The interactions between free surface nucleation and solid interface nucleation were reported to promote heterogeneous nucleation on the polyether ether ketone interface at high temperatures due to strong free-surface-induced recrystallization [50].

Due to the same interface chemistry, the interface environment also affects the crystal nucleation and growth process by changing the local supersaturation state. In general, at low concentrations, the crystallization process is more significantly affected by the chemical properties of the interface. Chemical functionality of the interface leads to specific interactions between these functional groups and solute molecules, resulting in the binding or reorientation of solutes at the interface. In contrast, at high concentrations, interfacial environmental factors dominate crystallization and affect the crystallization routes and structural evolution.

3.3 Rough structures and cavities

In addition to the chemical properties of the interface, the micro/nanostructure could also affect the crystallization process as the introduced nucleation site and regulation platform (Fig. 5). Rough structures and cavities are the simplest forms of nucleation sites [51–53]. On the ideal smooth surface, solute molecules are randomly adsorbed on the surface, migrate across the surface to form the first solute monolayer, and then grow layer by layer to form aggregates with appropriate bond angles. The aggregates gradually grow into clusters and then nucleate into crystals. When nucleation occurs on a rough surface, the rough structure could block the lateral migration of the adsorbed solute molecules so that solute molecules are trapped in the gap, forming a region of high local supersaturation and promoting crystal nucleation. Various rough interfaces have been constructed to form more cavities (Fig. 5(a)) [54].

The $\Delta G^*_{\mathrm{Heter}}$ is reduced by the presence of a rough structure due to the formation of cavities in solution and at the interface (Fig. 5(b)) [55], in which solute molecules gather to form a local supersaturation peak. Generally, cavities smaller than solute molecules could affect the crystallization process, while larger cavities have a similar effect as flat interfaces. Because protein molecules can aggregate, interfaces with cavities are conducive to protein supersaturation at low concentrations. Liu et al. used five kinds of polymers to treat glass slides, resulting in different surface roughnesses and uneven valley microstructures, which could induce heterogeneous nucleation of protein crystals and shorten the nucleation time (Fig. 5(c)) [5]. In addition, rough surfaces provide nucleation sites for protein crystals to reduce the nucleation barrier and induce the heterogeneous nucleation of protein crystals due to protein aggregation. In a further study on the effect of nucleation interfaces with different roughnesses on protein crystallization, the number of lysozyme and proteinase K crystals in the rough cover glass was determined to be higher than that in the control group [56]. Salehi et al. proved that the construction of a rough hydrogel interface effectively increased the local solute concentration, which was conducive to the enhancement of the Wenzel trend and the physical limitation of the rough hydrophilic surface, thus promoting protein nucleation to a greater extent [57].

Furthermore, improving the surface roughness is a key strategy for constructing a superhydrophobic interface. The rough micro/nanostructure could enhance the original hydrophilic or hydrophobic properties of the interface by increasing the number of cavities, thus changing the supersaturation state of solutes and regulating the

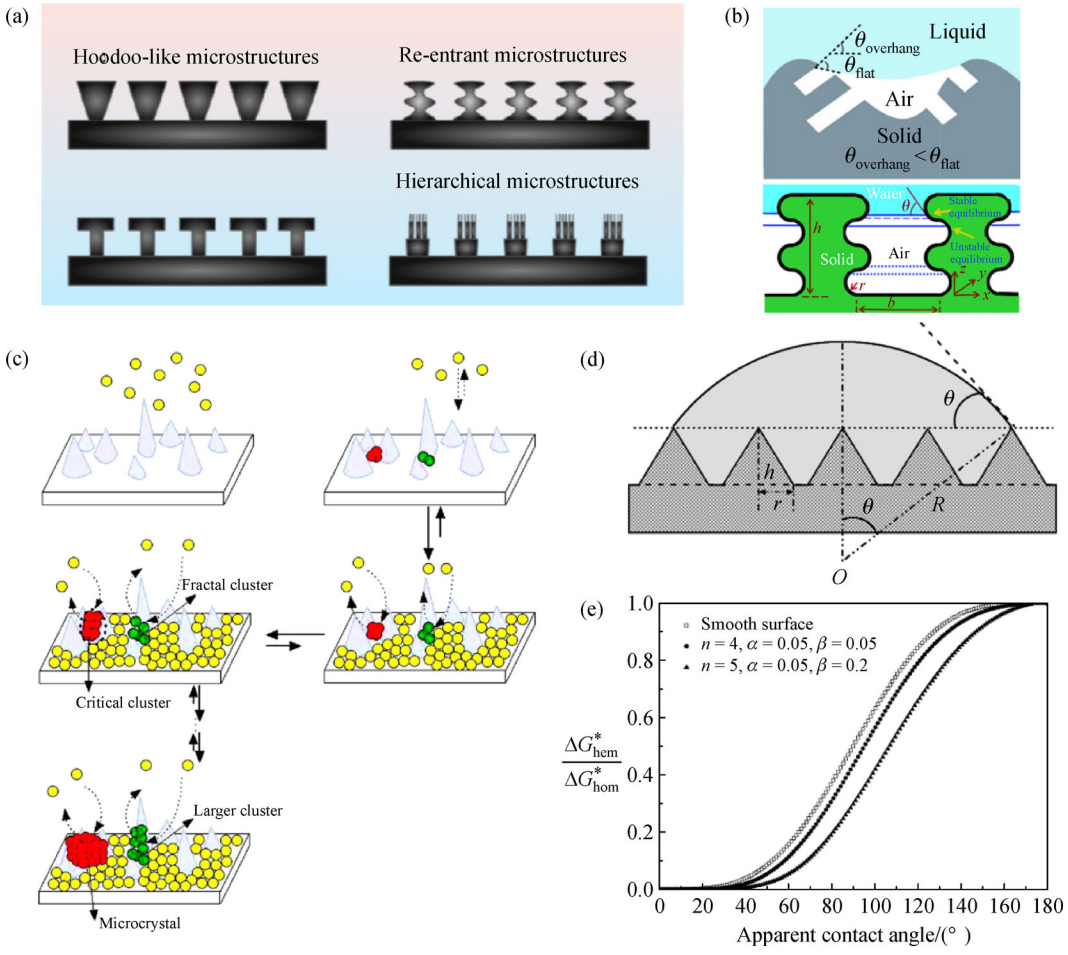

Fig. 5 (a) Various rough interfaces. Reprinted with permission from ref. [54], copyright 2016, Wiley. (b) Schematic cross-sectional profile of liquid in contact with a surface consisting of (top) overhang structures [58] and (bottom) re-entrant structures [59]. Reprinted with permission from ref. [58], copyright 2008, American Chemical Society (top), and ref. [59], copyright 2007, American Chemical Society (bottom). (c) Schematic illustration of protein crystallization and the formation of a large cluster on a rough surface. (d) Geometry of a sphere-cap-shaped nucleating solution on a rough surface. (e) Ratio as a function of the contact angle on different roughness. Reprinted with permission from ref. [5], copyright 2007, American Chemical Society.

nucleation of crystals. Liu et al. assumed that the rough surface consisted of a series of uniform cones (Fig. 5(d)) and corrected the formula for forming a nuclear barrier. The corrected formula is as follows [5]:

$$f(r,\theta)=\frac{\Delta G^{*}_{\text{Heter}}}{\Delta G^{*}_{\text{Homo}}}=\frac{1}{4}\frac{[2(1-\cos\theta)-\cos\theta(\sin\theta)^2]^3}{[(1-\cos\theta)^2(2+\cos\theta)+3\beta\sin\theta-n\alpha^2\beta^2]^2}, \tag{6}$$

$$\alpha=\frac{r}{R}, \tag{7}$$

$$\beta=\frac{h}{R}, \tag{8}$$

where R is the main radius of the spherical cap, and r, h, and n are the radius, height, and number of cones, respectively. As shown in Fig. 5(e), the experimental results showed that the time needed for heterogeneous nucleation induction of lysozyme crystals on a smooth surface was longer than that on a rough interface, which was consistent with the theoretical prediction.

3.4 Pore size and pore shape

The interfacial micropore is a special form of rough interface. For many compounds, interfacial micropores provide heterogeneous nucleation sites and guide the solute molecules in an orderly manner, leading to the rapid growth of initial nuclei along the long axis [60,61]. In metastable solutions, nanoscale pores endow the solute with nanoscale limitations, which can effectively control the nucleation kinetics and change the nucleation rate [62].

However, surface roughness alone is not a sufficient macroparameter for describing the effect of interfacial micropores on nucleation.

Recently, research on crystal nucleation in micro/nanopores has illustrated a significant influence on nucleation kinetics [63], polymorphism and crystal orientation (Fig. 6). During crystallization, the solution first condenses the capillaries in the pores and then nucleates rapidly. Capillarity affects the nucleation process by regulating the pore size of the interface. The nucleation rate is highest when the pore size is equal to the critical size of the initial nucleus. Nanoscale pores can provide additional sites through heterogeneous nucleation on the pore wall, which can promote the rapid aggregation of solute molecules to form critical nuclei, while larger micropores can provide more filled crystals as heterogeneous nucleation interfaces to promote crystal growth. Shah et al. prepared a series of ordered mesoporous templates to study the protein crystallization process [64]. As shown in Fig. 6(a), it was found that the crystallization of proteins strongly depended on the micropore size, which was directly related to the radius of gyration (R_g) for protein, and the proteins formed stable nuclei in pores of a specific size. Lu et al. reported that proteins confined to nanosized cylindrical pores exhibited a higher protein folding rate and improved thermodynamic stability with a decrease in pore size, which was close to twice the R_g of the proteins [65]. Diao et al. systematically changed the microstructures of polymer microgels to provide nanoconfinement, and the nucleation rate was significantly increased (Fig. 6(b)) [66]. Monte Carlo simulation of the nucleation indicated that there was an optimal pore size corresponding to the maximum nucleation rate, while improper pore size had no significant effect on nucleation

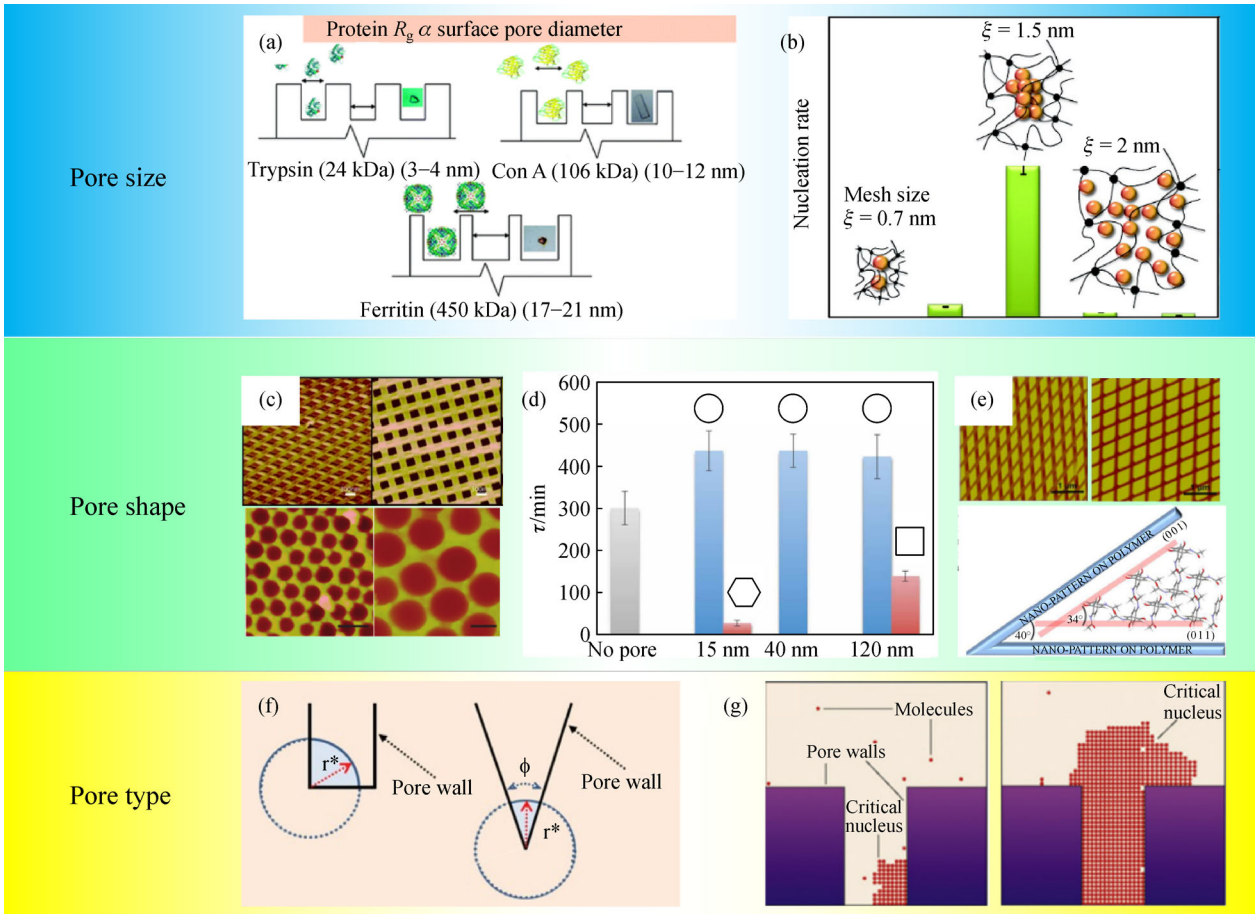

Fig. 6 (a) The ordered mesoporous templates to study the protein crystallization process. Reprinted with permission from ref. [64], copyright 2012, American Chemical Society. (b) The nucleation rate under confinement of a polymer mesh. Reprinted with permission from ref. [66], copyright 2011, American Chemical Society. (c) Atomic force microscope (AFM) images of spherical pores and square pores of the same size. Reprinted with permission from ref. [47], copyright 2011, Nature Publishing Group. (d) Effect of the nanopore shape in AA-co-DVB polymer films on the nucleation kinetics of aspirin. Reprinted with permission from ref. [47], copyright 2011, Nature Publishing Group. (e) AFM images of imprinted silicon masters and angle-directed nucleation. Reprinted with permission from ref. [67], copyright 2017, American Chemical Society. (f) Heterogeneous nucleation at the corner of rectangular pore and wedge-shaped pores. Reprinted with permission from ref. [68], copyright 2014, Wiley. (g) Crystal nucleation in a pore. Reprinted with permission from ref. [69], copyright 2006, Nature Publishing Group.

and crystallization.

To study the influence of interface pore shape on crystal nucleation, Diao et al. proposed controlling the surface pore geometry by nanoimprint lithography, specifically to modify the surface pattern aperture from a few nanometers to hundreds of nanometers, and they systematically studied the influence of different pore types on crystal nucleation (Fig. 6(c)) [47]. The average nucleation induction time of aspirin with different pore shape interfaces is shown in Fig. 6(d), which shows that the spherical nanopores hindered the nucleation of aspirin crystals, while the angular nanopores promoted nucleation. The orientation order of solutes in the near surface region could be improved by geometric constraints, which was conducive to the rearrangement of solute molecules in the process of crystal nucleation (Fig. 6(e)) [67]. The orientation of solutes in the near surface region increased with the enhancement of the pore angles, which was conducive to the rearrangement of solute molecules during nucleation. When the molecular orientation controlled by the angular geometry was similar to that in the crystal, the nucleation rate reached the maximum, and on the macroscopic scale, angular nucleation was apparent. However, it should be noted that the interaction between the interface and solute causes the influence of the pore shape on crystal nucleation.

The types of interface channels include rectangular pores and wedge-shaped pores (Fig. 6(f)) [68], which also affect the nucleation and growth process. As presented in Fig. 6(g), the crystal begins to grow at the corner of the rectangular pore until a critical molecular nucleus is formed [69]; this nucleus has been reported to induce the nucleation of crystals. The free energy barrier of wedge nucleation is related to the wedge angle, and the correction formula is as follows:

$$f(\theta,\phi)=\frac{\Delta G^{*}_{\mathrm{Heter}}}{\Delta G^{*}_{\mathrm{Homo}}}=\frac{1}{\pi}\Big[\cos\,\theta(\sin\,\theta)^{2}\sin\,\phi-\cos\,\theta\left(3-(\cos\,\theta)^{2}\phi+4\sin^{-1}\left(\sin\,\frac{\phi}{2}\sin\,\frac{\phi}{2}\right)\right)\Big], \quad (9)$$

where ϕ is the internal angle of the wedge.

3.5 Surface porosity

Surface porosity, calculated by the ratio of the pore area to the total surface area of interface, is the macroscopic expression of a porous micro/nanostructure at the interface, and it involves the pore size and quantity accumulation, which affects the mass transfer process and the local supersaturation of the interfacial solution [1,57,61,68,70], as shown in Fig. 7. According to the theoretical model of nucleation thermodynamics, an increase in porosity reduces the nuclear barrier, which is conducive to the rapid nucleation of crystals. Diao et al. reported that a nucleation interface with nanoscale porosity could increase the polar surface nucleation of aspirin by an order of magnitude [49]. Nindiyasari et al. studied the effects of different porosities on the crystallization of calcium carbonate in hydrogels, the surface morphology of which is shown in Fig. 7(a) [71]. It was found that the porosity changed the local supersaturation concentration of the interface by affecting the diffusion process of solutes in hydrogels. The relationship between the diffusion coefficient in the gel (D_{g}) and diffusion coefficient in water (D_{w}) is as follows:

$$D_{\mathrm{g}}=D_{\mathrm{W}}\left(\frac{\varepsilon}{\tau^{2}}\right), \quad (10)$$

where ε and τ are the porosity and the effective tortuosity of the hydrogel, respectively. Higher porosity and shorter diffusion column length led to an increase in the diffusion coefficient of solutes in hydrogels, resulting in nucleation at higher supersaturation levels of the interface to form various superstructures of calcium carbonate (Fig. 7(b)). Jo et al. prepared hydrogels with abundant surface porosities and polymer network structures to simulate ion transfer in organisms [72]. As the diffusion rate slowed, the flux of carbonate ions gradually decreased, resulting in the formation of various calcite structures along the diffusion direction; these structures were hopper-like, rosette-like and otoconia-like in order (Fig. 7(c)).

As mixed separation processes, membrane crystallization (MCr), which includes MDC [2,12,44,70], membrane cooling crystallization [73] and membrane antisolvent crystallization, is an important method of obtaining crystals with ideal particle size distribution. A microporous membrane is the core mass transfer device for the removal of concentrated solvents. The total porosity of the membrane is the main factor affecting the transmembrane flux [74,75]. The transfer characteristics of the membrane are closely related to its inherent micropore structure; such characteristics include the pore size, pore size distribution and channel curvature. The widely accepted Hagen-Poiseuille equation was used to describe the permeate flux (J) variation [76,77],

$$J=\frac{\varepsilon\pi r_{\mathrm{p}}^{2}\Delta p}{8\mu L}, \quad (11)$$

where r_{p} is the membrane pore radius; Δp, μ and L are the pressure gradient, liquid viscosity and length of the liquid flowing through the membrane, respectively. The high porosity showed lower transfer resistance and a larger mass transfer area, so that more solvent molecules could flow through the membrane at the same time. A change in the solvent concentration rate could effectively control the degree of supersaturation in the process, thus affecting the induction time needed for crystal nucleation, balancing the competition between crystal nucleation and growth and leading to the formation of ideal crystal products. Three different Hyflon/PVDF composite membranes were used

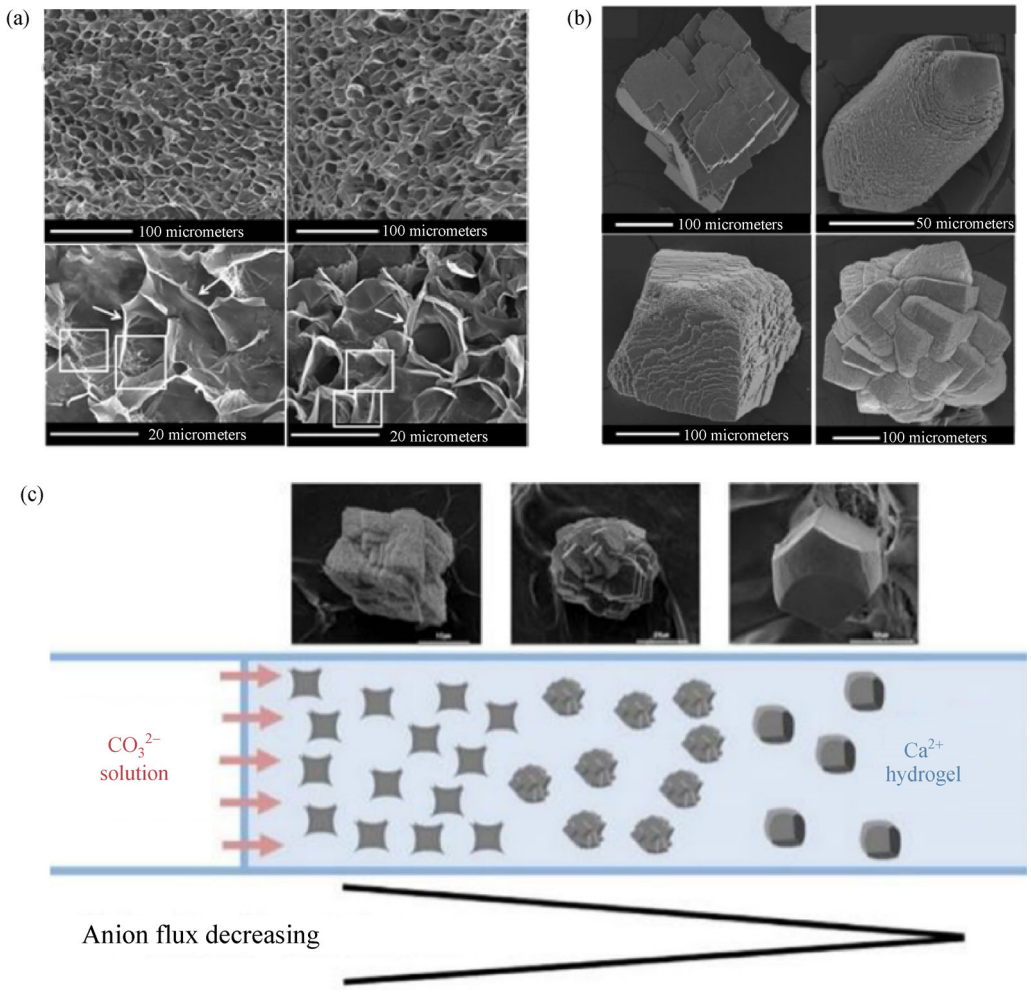

Fig. 7 (a) Scanning electron microscope (SEM) images illustrating the variation of the porosity of gelatin hydrogels. (b) SEM images of calcium carbonate with various superstructures. Reprinted with permission from ref. [71], copyright 2014, American Chemical Society. (c) Diffusion-controlled crystallization of calcium carbonate in a Hydrogel. Reprinted with permission from ref. [72], copyright 2019, American Chemical Society.

in the MCr experiments [74]. The maximum surface porosity and pore size of the composite membrane determined the maximum transmembrane flux, thus reducing the nucleation time and improving the crystal growth rate.

It is well known that the local concentration distribution of the environment near the interface affects the heterogeneous nucleation in the solution. As the porous interface can promote mass transfer of solvent, it could optimize the concentration distribution of the boundary layer by dispersing fluid over a short period of time and form a micron droplet dispersed phase [74,75]. Uniform interfacial properties are important for stabilizing the boundary layer concentration and regulating the crystallization route and structural evolution. Similarly, the interface, as the main site of heat transfer, would also affect the interface temperature distribution. Crystallization, an exothermic process, changes the state from a high-energy disordered solution to a low-energy crystal. An interface with high thermal conductivity is conducive to heat transfer to maintain the stable temperature distribution of the interface at different times [73]. In addition, the interface temperature distribution also depends on the specific surface area of the interface. A higher specific surface is more conducive to an efficient heat transfer process. In particular, in the cooling crystallization process, efficient heat exchange at the interface helps to quickly establish the undercooling interface and effectively promote nucleation [73]. Compared with traditional cooling crystallization, heterogeneous nucleation at the uniform interface is conducive to obtaining a uniform interfacial concentration/temperature distribution to improve the uniformity of the particle size distribution and lay a foundation for the development of new crystallization technology.

3.6 Channels on the interface

The channels on the interface, which can be divided into through channels and dead end channels (Fig. 8), are used to control mass transfer during the crystallization process, which is a further embodiment of intensifying the local supersaturation of porous micro/nano interfaces [78,79]. In one study, through channels were used as heterogeneous nucleation interfaces and separation interfaces to concentrate the solvent and control the supersaturation at the interface, thus achieving the simultaneous improvement of solvent recovery and crystal product quality. Appropriate supersaturation is conducive to the formation of crystals with complete crystal shapes and smooth surfaces. The effective removal of solvent by interfacial channels is conducive to the rapid separation of solvent and solute, thus inducing crystallization.

A microporous membrane is a typical representative of a through channel structure. Mass transfer in the membrane channel is realized by convection and diffusion of the solvent. The driving forces of mass transfer are pressure differences, temperature differences or concentration differences between the two sides of the membrane. There are three mass transfer models for microporous membranes: Knudsen diffusion, molecular diffusion and viscous flow diffusion (Fig. 8(a)) [80]. Knudsen diffusion, based on collisions between the molecule and the pore wall, plays a dominant role when r_p is less than the average molecular free path (r_m). In contrast, molecular diffusion is based on intermolecular collisions, as the r_p is much larger than r_m. Viscous flow diffusion, also known as Poiseuille flow, is based on intermolecular collisions and molecule-wall collisions. The Poiseuille flow model is dominant when the membrane pore size is larger than the average free molecular path [81]. The characteristics of the membrane channel, including the pore size, porosity, tortuosity and thickness, could affect the mass transfer. The pore size of the microporous membranes for MCr is usually larger than the free path of the molecular motion of the solute; that is, the molecular flow in pores mainly undergoes intermolecular collision, and the transfer characteristics are between the Knudsen flow ($r_p < r_m$) and viscous flow ($r_p \gg r_m$) models. According to the Hagen-Poiseuille formula [81], the standard volume flow (Q_V) through the interfacial crystallizer pore can be obtained. The formula is as follows,

$$Q_V = \frac{NRT}{P} = \frac{\pi r_p^4 p^* \Delta p}{8T^* \mu L \tau}, \tag{12}$$

where L and τ are the thickness and tortuosity factor of the membrane, respectively. The increase in thickness and tortuosity could increase the mass transfer resistance. Commercial microfiltration membranes with uneven pore radii and high τ (Fig. 8(b)) show different mass transfer

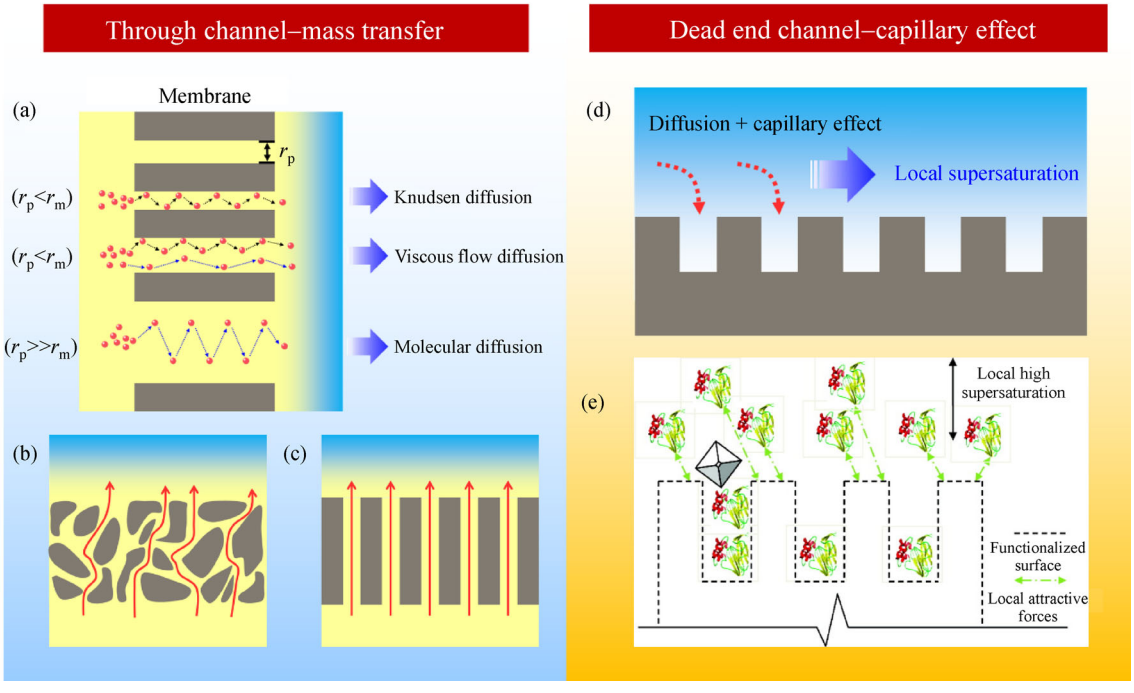

Fig. 8 Schematic diagram of three mass transfer models: (a) Knudsen diffusion, molecular diffusion and viscous flow diffusion; (b) commercial microfiltration membranes with uneven r_p and high τ; (c) ideal straight through channel with uniform r_p and τ of 1; (d) solute molecules enter the nanoscale channel under the combined action of diffusion and capillary effect; (e) crystallization of proteins at ultralow supersaturations using 3D nano-templates. Reprinted with permission from ref. [84], copyright 2012, American Chemical Society.

rates in the channel, which easily leads to uneven distribution of local supersaturation concentrations, resulting in explosive nucleation and poor crystal morphologies. The ideal straight through channel (Fig. 8(c)) is expected to have a uniform r_p and τ of 1 to increase the mass transfer efficiency and realize the directional preparation of crystals.

In dead end channels, solute molecules enter the nanoscale channel under the combined action of diffusion and capillary effects [82,83], which effectively increase the local supersaturation concentration of the solute and further promote the nucleation process (Fig. 8(d)). The high local supersaturation of biomacromolecules with confinement is the thermodynamic driving force for nucleation in pores [47]. The solution condenses capillaries in the confined nanopores and then undergoes rapid nucleation. The maximum nucleation rate is obtained when the pore size is equal to the size of the critical nucleus of the biomacromolecule. Shah et al. prepared a series of ordered mesoporous templates with dead end channels and successfully crystallized concanavalin A, human serum albumin and ferritin on porous substrates for the first time [64]. In addition, a series of novel three-dimensional (3D) nano templates with adjustable surface mesopores and surface chemistry were developed to promote protein crystallization through the use of dead end channels (Fig. 8(e)) [84], which provided a targeting strategy for the structure determination of high-value proteins.

3.7 Interface properties in process intensification

The application of interface properties in process intensification is mainly reflected in shortening the crystal induction period and strengthening the mass transfer through the regulation of interface chemicals and micro/nanostructures to realize the rapid nucleation of crystals. Diao et al. effectively shortened the induction time of aspirin and induced the preferred orientation nucleation of aspirin by using the interactions between the polymer membrane and solute [47]. In addition, polymer microgels with tunable chemical surface structures were also reported by Diao's group to investigate the intermolecular interactions limiting nucleation and controlling crystallization, resulting in a nucleation kinetics enhancement of four orders of magnitude [48]. The interaction between the polymer and solute controls the nucleation kinetics and induces rapid nucleation. In addition to the interaction between the interface and solute, the micro/nanostructure can also shorten the nucleation induction period. Liu et al. proved that different surface roughnesses and uneven valley microstructures could induce heterogeneous nucleation of protein crystals and shorten the nucleation time [5].

In addition, the realization of efficient micro-mixing through enhanced mass transfer is an important part of the application of interface properties in process intensification and is mainly affected by interfacial porosity and channels. Increasing the porosity and mass transfer area could effectively reduce the mass transfer resistance so that more solvent molecules flow through the interface at the same time [76,77]. The change in solvent concentration rate could effectively control the degree of supersaturation in the process, thus affecting the induction time of crystal nucleation to balance the competition between crystal nucleation and growth and obtain ideal crystal products. In addition, the through channel was used as both a heterogeneous nucleation interface and separation interface to concentrate the solvent and control the supersaturation at the interface, thus achieving the simultaneous improvement of solvent recovery and crystal product quality. The preparation of an ideal straight-through channel with a uniform r_p and τ of 1 is a future development direction to realize efficient process intensification.

Prior to microscale crystallization, microfluidics technology, microforce fields, and microscale intensified mass transfer processes based on membrane technology could achieve molecular mixing, which has a decisive impact on improving the morphology and purity of crystal particles [85–88]. The construction and design of microscale mixing and transfer processes in confined space could make the mixing and transfer effects in different regions consistent within a short period of time. In contrast to other mass transfer process intensifications, the efficient mixing transfer efficiency of membranes has excellent performance due to submicron scale channels and can realize the coupling of crystal nucleation and growth processes to meet the needs of directional growth regulation of crystal size and morphology [88].

4 Conclusions and perspectives

With the development of crystallization nucleation theory and interface control methods, the heterogeneous nucleation process induced by interfaces is the cross frontier of engineering, and materials are an area of high research interest. At present, research has proven the feasibility of interface properties, including chemical properties (hydrophobicity and functional group) and micro/nanostructures (rough structures and cavities, pore shape and pore size, surface porosity, and channels) in the regulation of the crystallization process and has made great progress in expanding the theory of crystallization and nucleation.

Interface properties could shorten the crystal induction period and enhance mass transfer by adjusting the interface chemistry and micro/nanostructure to realize the rapid nucleation of crystals. The hydrophobic interactions and functional groups could effectively regulate the solute concentration at the interface and induce rapid nucleation. In contrast, the micro/nanostructures could not only provide heterogeneous nucleation sites but also guide the orderly growth of solute molecules. The porous interface

has been used as a heterogeneous nucleation interface and separation interface to concentrate the solvent and control the supersaturation at the interface, thus achieving the simultaneous improvement of solvent recovery and crystal product quality. In addition, the homogeneity of the interfacial chemical structure and micro/nanostructure is a prerequisite to ensure its influence on crystallization. However, the mechanism of crystallization nucleation and targeted preparation of crystals via diverse interfacial structures at the microscale remains to be elucidated.

In the future, research on the regulation of the interface crystallization process will focus on the following aspects: 1) The theory of interface characteristic design still needs to be elucidated, as this theory is the key to realizing targeted crystal preparation. 2) A uniform interface crystallizer with the functions of crystallization control and accurate mass transfer should be constructed to meet the requirements of continuous and scale-up crystallizers, thus achieving the demands of pharmaceutical crystallization and fine chemical preparation. 3) The expansion of the types of proper interface materials and the development of intelligent interfaces with more functions can meet the needs of different crystallization systems. 4) Finally, an important goal is to master a simplified method of providing a customized interface for each new molecule to be crystallized to improve the universality.

Acknowledgements We acknowledge the financial contribution from Creative Research Groups of the National Natural Science Foundation of China (Grant No. 22021005), National Natural Science Foundation of China (Grant Nos. 21978037 and 21978033), Fundamental Research Funds for the Central Universities (Grant No. DUT19TD33), and National Key Research and Development Program of China (Grant No. 2019YFE0119200), Support Plan of Innovative Talents of Liaoning Province (Grant Nos. XLYC1901005, XLYC1907149, XLYC1907063), Dalian Innovative Science and Technology Fund (Grant Nos. 2020JJ26SN064 and 2021JJ12GX019).

References

1. Shah U V, Amberg C, Diao Y, Yang Z, Heng J Y Y. Heterogeneous nucleants for crystallogenesis and bioseparation. Current Opinion in Chemical Engineering, 2015, 8: 69–75
2. Jiang X, Shao Y, Li J, Wu M, Niu Y, Ruan X, Yan X, Li X, He G. Bioinspired hybrid micro/nanostructure composited membrane with intensified mass transfer and antifouling for high saline water membrane distillation. ACS Nano, 2020, 14(12): 17376–17386
3. Bi Y, Cabriolu R, Li T. Heterogeneous ice nucleation controlled by the coupling of surface crystallinity and surface hydrophilicity. Journal of Physical Chemistry C, 2016, 120(3): 1507–1514
4. Wu Q, Gao A, Tao F, Yang P. Understanding biomolecular crystallization on amyloid-like superhydrophobic biointerface. Advanced Materials Interfaces, 2018, 5(6): 1701065
5. Liu Y X, Wang X J, Lu J, Ching C B. Influence of the roughness, topography, and physicochemical properties of chemically modified surfaces on the heterogeneous nucleation of protein crystals. Journal of Physical Chemistry B, 2007, 111(50): 13971–13978
6. Curcio E, Curcio V, Profio G D, Fontananova E, Drioli E. Energetics of protein nucleation on rough polymeric surfaces. Journal of Physical Chemistry B, 2010, 114(43): 13650–13655
7. Paxton T E, Sambanis A, Rousseau R W. Influence of vessel surfaces on the nucleation of protein crystals. Langmuir, 2001, 17 (10): 3076–3079
8. Wang M, Liu G, Yu H, Lee S H, Wang L, Zheng J, Wang T, Yun Y, Lee J K. ZnO nanorod array modified PVDF membrane with superhydrophobic surface for vacuum membrane distillation application. ACS Applied Materials & Interfaces, 2018, 10(16): 13452–13461
9. Jiang X, Tuo L, Lu D, Hou B, Chen W, He G. Progress in membrane distillation crystallization: process models, crystallization control and innovative applications. Frontiers of Chemical Science and Engineering, 2017, 11(4): 647–662
10. Leaper S, Abdel-Karim A, Gorgojo P. The use of carbon nanomaterials in membrane distillation membranes: a review. Frontiers of Chemical Science and Engineering, 2021, 15(4): 755–774
11. Rehman W U, Muhammad A, Younas M, Wu C, Hu Y, Li J. Effect of membrane wetting on the performance of PVDF and PTFE membranes in the concentration of pomegranate juice through osmotic distillation. Journal of Membrane Science, 2019, 584: 66–78
12. Liu C, Chen L, Zhu L. Fouling mechanism of hydrophobic polytetrafluoroethylene (PTFE) membrane by differently charged organics during direct contact membrane distillation (DCMD) process: an especial interest in the feed properties. Journal of Membrane Science, 2018, 548: 125–135
13. Saffarini R B, Mansoor B, Thomas R, Arafat H A. Effect of temperature-dependent microstructure evolution on pore wetting in PTFE membranes under membrane distillation conditions. Journal of Membrane Science, 2013, 429: 282–294
14. Shao Y, Han M, Wang Y, Li G, Xiao W, Li X, Wu X, Ruan X, Yan X, He G, Jiang X. Superhydrophobic polypropylene membrane with fabricated antifouling interface for vacuum membrane distillation treating high concentration sodium/magnesium saline water. Journal of Membrane Science, 2019, 579: 240–252
15. Wang Y, He G, Shao Y, Zhang D, Ruan X, Xiao W, Li X, Wu X, Jiang X. Enhanced performance of superhydrophobic polypropylene membrane with modified antifouling surface for high salinity water treatment. Separation and Purification Technology, 2019, 214: 11–20
16. Lv J, Song Y, Jiang L, Wang J. Bio-inspired strategies for anti-icing. ACS Nano, 2014, 8(4): 3152–3169
17. Eberle P, Tiwari M K, Maitra T, Poulikakos D. Rational nanostructuring of surfaces for extraordinary icephobicity. Nanoscale, 2014, 6(9): 4874–4881
18. Zhang Z, Liu X Y. Control of ice nucleation: freezing and antifreeze strategies. Chemical Society Reviews, 2018, 47(18): 7116–7139
19. Tang Y, Zhang Q, Zhan X, Chen F. Superhydrophobic and anti-icing properties at overcooled temperature of a fluorinated hybrid surface prepared via a sol-gel process. Soft Matter, 2015, 11(22): 4540–4550
20. Meuler A J, Mckinley G H, Cohen R E. Exploiting topographical texture to impart icephobicity. ACS Nano, 2010, 4(12): 7048–7052

21. Nanev C N, Saridakis E, Govada L, Kassen S C, Solomon H V, Chayen N E. Hydrophobic interface-assisted protein crystallization: theory and experiment. ACS Applied Materials & Interfaces, 2019, 11(13): 12931–12940
22. Nanev C. Protein crystal nucleation: recent notions. Crystal Research and Technology, 2007, 42(1): 4–12
23. Nanev C. Recent insights into protein crystal nucleation. Crystals, 2018, 8(219): 1–12
24. Nanev C. Peculiarities of protein crystal nucleation and growth. Crystals, 2018, 8(422): 1–16
25. Pham T, Lai D, Ji D, Tuntiwechapikul W, Friedman J M, Lee T R. Well-ordered self-assembled monolayer surfaces can be used to enhance the growth of protein crystals. Colloids and Surfaces. B, Biointerfaces, 2004, 34(3): 191–196
26. D'Arcy A, Sweeney A M, Haber A. Using natural seeding material to generate nucleation in protein crystallization experiments. Acta Crystallographica. Section D, Biological Crystallography, 2003, D59(7): 1343–1346
27. Boinovich L B, Emelyanenko A M. Hydrophobic materials and coatings: principles of design, properties and applications. Russian Chemical Reviews, 2008, 77(7): 583–600
28. Brassard J D, Sarkar D K, Perron J. Fluorine based superhydrophobic coatings. Applied Sciences (Basel, Switzerland), 2012, 2(2): 453–464
29. Li L, Li B, Dong J, Zhang J. Roles of silanes and silicones in forming superhydrophobic and superoleophobic materials. Journal of Materials Chemistry. A, Materials for Energy and Sustainability, 2016, 4(36): 13677–13725
30. Xiao Z, Zheng R, Liu Y, He H, Yuan X, Ji Y, Li D, Yin H, Zhang Y, Li X M, He T. Slippery for scaling resistance in membrane distillation: a novel porous micropillared superhydrophobic surface. Water Research, 2019, 155: 152–161
31. Song Y Y, Felix S S, Bauer S, Schmuki P. Amphiphilic TiO_2 nanotube arrays: an actively controllable drug delivery system. Journal of the American Chemical Society, 2009, 131(12): 4230–4232
32. Fan X, Su Y, Zhao X, Li Y, Zhang R, Ma T, Liu Y, Jiang Z. Manipulating the segregation behavior of polyethylene glycol by hydrogen bonding interaction to endow ultrafiltration membranes with enhanced antifouling performance. Journal of Membrane Science, 2016, 499: 56–64
33. Chang Y, Ko C Y, Shih Y J, Quémener D, Deratani A, Wei T C, Wang D M, Lai J Y. Surface grafting control of PEGylated poly (vinylidene fluoride) antifouling membrane via surface-initiated radical graft copolymerization. Journal of Membrane Science, 2009, 345(1-2): 160–169
34. Chen L H, Huang A, Chen Y R, Chen C H, Hsu C C, Tsai F Y, Tung K L. Omniphobic membranes for direct contact membrane distillation: effective deposition of zinc oxide nanoparticles. Desalination, 2018, 428: 255–263
35. Dong Y, Ma L, Tang C Y, Yang F, Quan X, Jassby D, Zaworotko M J, Guiver M D. Stable superhydrophobic ceramic-based carbon nanotube composite desalination membranes. Nano Letters, 2018, 18(9): 5514–5521
36. Liu Y, Su Y, Cao J, Guan J, Zhang R, He M, Fan L, Zhang Q, Jiang Z. Antifouling, high-flux oil/water separation carbon nanotube membranes by polymer-mediated surface charging and hydrophilization. Journal of Membrane Science, 2017, 542: 254–263
37. Dixit D, Ghoroi C. Role of randomly distributed nanoscale roughness for designing highly hydrophobic particle surface without using low surface energy coating. Journal of Colloid and Interface Science, 2020, 564: 8–18
38. Mohammadi E, Qu G, Kafle P, Jung S H, Lee J K, Diao Y. Design rules for dynamic-template-directed crystallization of conjugated polymers. Molecular Systems Design & Engineering, 2020, 5(1): 125–138
39. Curcio E, López-Mejías V, Di Profio G, Fontananova E, Drioli E, Trout B L, Myerson A S. Regulating nucleation kinetics through molecular interactions at the polymer–solute interface. Crystal Growth & Design, 2014, 14(2): 678–686
40. Wang Z, Dong X, Liu G, Xing Q, Cavallo D, Jiang Q, Müller A J, Wang D. Interfacial nucleation in iPP/PB-1 blends promotes the formation of polybutene-1 trigonal crystals. Polymer, 2018, 138: 396–406
41. Flieger A K, Schulz M, Thurn-Albrecht T. Interface-induced crystallization of polycaprolactone on graphite via first-order prewetting of the crystalline phase. Macromolecules, 2017, 51(1): 189–194
42. Kim H, Hong J, Kim C, Shin E Y, Lee M J, Noh Y Y, Park B C, Hwang I. Impact of hydroxyl groups boosting heterogeneous nucleation on perovskite grains and photovoltaic performances. Journal of Physical Chemistry C, 2018, 122(29): 16630–16638
43. López-Mejías V, Myerson A S, Trout B L. Geometric design of heterogeneous nucleation sites on biocompatible surfaces. Crystal Growth & Design, 2013, 13(8): 3835–3841
44. Macedonio F, Politano A, Drioli E, Gugliuzza A. Bi_2Se_3-assisted membrane crystallization. Materials Horizons, 2018, 5(5): 912–919
45. Suzuki H, Takiyama H. Observation and evaluation of crystal growth phenomena of glycine at the template interface with L-leucine. Advanced Powder Technology, 2016, 27(5): 2161–2167
46. Tsekova D S, Williams D R, Heng J Y Y. Effect of surface chemistry of novel templates on crystallization of proteins. Chemical Engineering Science, 2012, 77: 201–206
47. Diao Y, Harada T, Myerson A S, Hatton T A, Trout B L. The role of nanopore shape in surface-induced crystallization. Nature Materials, 2011, 10(11): 867–871
48. Diao Y, Helgeson M E, Siam Z A, Doyle P S, Myerson A S, Hatton T A, Trout B L. Nucleation under soft confinement: role of polymer–solute interactions. Crystal Growth & Design, 2011, 12(1): 508–517
49. Diao Y, Myerson A S, Hatton T A, Trout B L. Surface design for controlled crystallization: the role of surface chemistry and nanoscale pores in heterogeneous nucleation. Langmuir, 2011, 27 (9): 5324–5334
50. Luo S, Kui X, Xing E, Wang X, Xue G, Schick C, Hu W, Zhuravlev E, Zhou D. Interplay between free surface and solid interface nucleation on two-step crystallization of poly(ethylene terephthalate) thin films studied by fast scanning calorimetry. Macromolecules, 2018, 51(14): 5209–5218
51. Grosfils P, Lutsko J F. Impact of surface roughness on crystal nucleation. Crystals, 2020, 11(4): 1–20
52. Abyzov A S, Schmeizer J W P, Davydov L N. Heterogeneous

nucleation on rough surfaces: generalized Gibbs' approach. Journal of Chemical Physics, 2017, 147(21): 214705
53. Yan D, Zeng Q, Xu S, Zhang Q, Wang J. Heterogeneous nucleation on concave rough surfaces: thermodynamic analysis and implications for nucleation design. Journal of Physical Chemistry C, 2016, 120(19): 10368–10380
54. Su B, Tian Y, Jiang L. Bioinspired interfaces with superwettability: from materials to chemistry. Journal of the American Chemical Society, 2016, 138(6): 1727–1748
55. Liu K, Cao M, Fujishima A, Jiang L. Bio-inspired titanium dioxide materials with special wettability and their applications. Chemical Reviews, 2014, 114(19): 10044–10094
56. Karthika S, Radhakrishnan T K, Kalaichelvi P. A review of classical and nonclassical nucleation theories. Crystal Growth & Design, 2016, 16(11): 6663–6681
57. Salehi S M, Manjua A C, Belviso B D, Portugal C A M, Coelhoso I M, Mirabelli V, Fontananova E, Caliandro R, Crespo J G, Curcio E, et al. Hydrogel composite membranes incorporating iron oxide nanoparticles as topographical designers for controlled heteronucleation of proteins. Crystal Growth & Design, 2018, 18(6): 3317–3327
58. Cao L, Price T P, Weiss M, Gao D. Super water- and oil-repellent surfaces on intrinsically hydrophilic and oleophilic porous silicon films. Langmuir, 2008, 24(5): 1640–1643
59. Nosonovsky M. Multiscale roughness and stability of superhydrophobic biomimetic interfaces. Langmuir, 2007, 23(6): 3157–3161
60. Nanev C N, Saridakis E, Chayen N E. Protein crystal nucleation in pores. Scientific Reports, 2017, 7(1): 35821
61. Pach E, Verdaguer A. Pores dominate ice nucleation on feldspars. Journal of Physical Chemistry C, 2019, 123(34): 20998–21004
62. Wei P S, Hsiao S Y. Effects of supersaturation on pore shape in solid. Journal of Crystal Growth, 2017, 460: 126–133
63. Chayen N E, Saridakis E, Sear R P. Experiment and theory for heterogeneous nucleation of protein crystals in a porous medium. Proceedings of the National Academy of Sciences of the United States of America, 2006, 103(3): 597–601
64. Shah U V, Williams D R, Heng J Y Y. Selective crystallization of proteins using engineered nanonucleants. Crystal Growth & Design, 2012, 12(3): 1362–1369
65. Lu D, Liu Z, Wu J. Structural transitions of confined model proteins: molecular dynamics simulation and experimental validation. Biophysical Journal, 2006, 90(9): 3224–3238
66. Diao Y, Helgeson M E, Myerson A S, Hatton T A, Doyle P S, Trout B L. Controlled nucleation from solution using polymer microgels. Journal of the American Chemical Society, 2011, 133(11): 3756–3759
67. Stojaković J, Baftizadeh F, Bellucci M A, Myerson A S, Trout B L. Angle-directed nucleation of paracetamol on biocompatible nanoimprinted polymers. Crystal Growth & Design, 2017, 17(6): 2955–2963
68. Asanithi P. Surface porosity and roughness of micrographite film for nucleation of hydroxyapatite. Journal of Biomedical Materials Research. Part A, 2014, 102(8): 2590–2599
69. Frenkel D. Seeds of phase change. Nature, 2006, 443(7112): 641
70. Meng S, Ye Y, Mansouri J, Chen V. Fouling and crystallisation behaviour of superhydrophobic nano-composite PVDF membranes in direct contact membrane distillation. Journal of Membrane Science, 2014, 463: 102–112
71. Nindiyasari F, Fernández-Díaz L, Griesshaber E, Astilleros J M, Sánchez-Pastor N, Schmahl W W. Influence of gelatin hydrogel porosity on the crystallization of $CaCO_3$. Crystal Growth & Design, 2014, 14(4): 1531–1542
72. Jo M K, Oh Y, Kim H J, Kim H L, Yang S H. Diffusion-controlled crystallization of calcium carbonate in a hydrogel. Crystal Growth & Design, 2019, 20(2): 560–567
73. Jiang X, Lu D, Xiao W, Ruan X, Fang J, He G. Membrane assisted cooling crystallization: process model, nucleation, metastable zone, and crystal size distribution. AIChE Journal. American Institute of Chemical Engineers, 2016, 62(3): 829–841
74. Cui Z, Li X, Zhang Y, Wang Z, Gugliuzza A, Militano F, Drioli E, Macedonio F. Testing of three different PVDF membranes in membrane assisted-crystallization process: influence of membrane structural-properties on process performance. Desalination, 2018, 440: 68–77
75. Ko C C, Ali A, Drioli E, Tung K L, Chen C H, Chen Y R, Macedonio F. Performance of ceramic membrane in vacuum membrane distillation and in vacuum membrane crystallization. Desalination, 2018, 440: 48–58
76. Hong X, Huang X J, Gao Q L, Wu H M, Guo Y Z, Huang F, Fang F, Huang H T, Chen D J. Microstructure-performance relationships of hollow-fiber membranes with highly efficient separation of oil-in-water emulsions. Journal of Applied Polymer Science, 2019, 136 (23): 47615
77. Gao S, Shi Z, Zhang W B, Zhang F, Jin J. Photo-induced superwetting single-walled carbon nanotube/TiO_2 ultrathin network films for ultrafast separation of oil-in-water emulsions. ACS Nano, 2014, 8(6): 6344–6352
78. Fang A, Hailey A K, Grosskopf A, Anthony J E, Loo Y L, Haataj M. Capillary effects in guided crystallization of organic thin films. APL Materials, 2015, 3(036107): 036107
79. Ahmad F, Rahimi A, Tsotsas E, Prat M, Kharaghani A. From micro-scale to macro-scale modeling of solute transport in drying capillary porous media. International Journal of Heat and Mass Transfer, 2021, 165: 120722
80. Mandiang Y, Sene M, Thiam A, Azillinon D. Daily estimate of pure water in a desalination unit by solar membrane distillation. Journal of Marine Science and Engineering, 2015, 4(3): 1–7
81. Cai J, Perfect E, Cheng C L, Hu X. Generalized modeling of spontaneous imbibition based on Hagen-Poiseuille flow in tortuous capillaries with variably shaped apertures. Langmuir, 2014, 30(18): 5142–5151
82. Vincent O, Zhang J, Choi E, Zhu S, Stroock A D. How solutes modify the thermodynamics and dynamics of filling and emptying in extreme ink-bottle pores. Langmuir, 2019, 35(8): 2934–2947
83. Desgranges C, Delhommelle J. Nucleation of capillary bridges and bubbles in nanoconfined CO_2. Langmuir, 2019, 35(47): 15401–15409
84. Shah U V, Allenby M C, Williams D R, Heng J Y Y. Crystallization of proteins at ultralow supersaturations using novel three-dimensional nanotemplates. Crystal Growth & Design, 2012, 12(4): 1772–1777

85. Jensen K F. Flow chemistry—microreaction technology comes of age. AIChE Journal. American Institute of Chemical Engineers, 2017, 63(3): 858–869
86. Koizumi H, Fujiwara K, Uda S. Role of the electric double layer in controlling the nucleation rate for tetragonal hen egg white lysozyme crystals by application of an external electric field. Crystal Growth & Design, 2010, 10(6): 2591–2595
87. Bhangu S K, Ashokkumar M, Lee J. Ultrasound assisted crystallization of paracetamol: crystal size distribution and polymorph control. Crystal Growth & Design, 2016, 16(4): 1934–1941
88. Tuo L, Ruan X, Xiao W, Li X, He G, Jiang X. A novel hollow fiber membrane-assisted antisolvent crystallization for enhanced mass transfer process control. AIChE Journal. American Institute of Chemical Engineers, 2019, 65(2): 734–744